sufficient to remove much of the excess rotational and vibrational energy present due to the ionization process. Approach to equilibrium was followed from endoergic and exoergic directions. Prior to reaction, one of the parent ions was ejected from the reaction cell and the population change of both parent ions was monitored at set time intervals. Equilibrium was deemed to have been achieved when the ratio of the two parent ion populations reached a constant value within experimental error.

Partial pressures of the various neutrals were determined by using an ion gauge calibrated with an MKS baratron capacitance manometer (in the 10^{-5} Torr range) extrapolated to experimental conditions. In order to approach dynamic pressure equilibrium throughout the vacuum chamber, the 300 L s^{-1} pumping speed of the diffusion pump connected to the high-vacuum chamber was reduced to ca. 75 L s^{-1}. Neutral gas pressures were calibrated for all reactants in open (75 L s^{-1}) and closed (no pumping) systems. It has been shown that partial pressure is independent of neutral gas leak rate.[49] A calibrated ion gauge connected to a Granville-Phillips controller was positioned at the site of the reaction cell with the magnetic field off, thus providing a field free vacuum system. The pressure measured at the middle of the vacuum chamber where the reaction cell is located, was equivalent to metallocene pressures determined at the remote ion gauge following pressure calibrations.[49]

Temperature Dependence. The temperature dependencies of electron-transfer equilibria were investigated by using a customized cell heater designed to heat a 1" × 1" × $1^3/_4$" analyzer cell. The heater consisted of two Macor plates ($1^1/_2$" × 2" × $^1/_4$") (Astro Met Inc.) attached to the long sides of the reaction cell. Ni-Cu wire (0.015" diameter, Omega) was wrapped around the external Macor plates and was resistively heated by using an Omega digital temperature controller (up to temperatures of up to 520 K). Cell temperatures were measured by using an Omega RTD thin film detector fastened to the analyzer cell. Additionally, the entire high-vacuum chamber was heated by using the vacuum bake-out system in order to minimize radiative temperature loss to the vacuum chamber walls.

Following the measurement of K_{eq} at a set temperature, the cell heater and bake-out were allowed to cool to a lower temperature and the entire system was allowed to equilibrate at the new temperature for 30 min. Experimental reproducibility was then tested by following the temperature dependence of K_{eq} as the reaction cell temperature was increased from 350 to 500 K. Cell temperature was measured before and after each reaction and usually fluctuated ±2 K during a single experiment. Typically, reactions were repeated three times at a single temperature. Linear regression and statistical analyses of the all measured equilibrium constants provided error limits at the 95% confidence level for reported $\Delta H_{e1}°$ and $\Delta S_{e1}°$ values.

Compounds. Metallocenes were purchased through Strem Chemicals except for ferrocene and ruthenocene (Aldrich). No further purification was required except for Cp_2Mn, which was resublimed prior to use. Organic reference compounds were purchased from Aldrich except *N*,*N*-diethyl-*p*-toluidine (Alfa Chemicals). A sample of 1,1'-bipyrrolidine[14c] was donated by Professor Stephen Nelsen (U. Wisconsin). Organic reference compounds were used without further purification. Liquid samples were degassed through several freeze-pump-thaw cycles prior to use.

Far-Infrared Spectroscopy. Ferrocene salts in Table II were prepared according to literature procedures.[22a,32] The samples were prepared as dilute 13-mm polyethylene pellets. Far-infrared spectra were recorded using a Bruker IFS 113 V spectrophotometer in the 50-750 cm^{-1} spectral region.

Acknowledgment. This work was supported by a grant from the National Science Foundation (CHE 9008663). The authors are grateful to Professor Nelsen and Peter A. Petillo for donation of the alkylhydrazine reference compound. The assistance of Professor William Weltner and Dr. San Li with the measurement of far-IR spectra is gratefully acknowledged. Professor M. Weaver kindly brought ref 47 to our attention.

(49) (a) Bruce, J. E.; Ryan, M. F. Unpublished Results. (b) Bruce, J. E.; Eyler, J. R. *J. Am. Soc. Mass Spectrom.*, in press.

Trimethyl Phosphate: The Intrinsic Reactivity of Carbon versus Phosphorus Sites with Anionic Nucleophiles

Rachel C. Lum[†] and Joseph J. Grabowski*[,‡]

Contribution from the Departments of Chemistry, Harvard University, Cambridge, Massachusetts 02138, and University of Pittsburgh, Pittsburgh, Pennsylvania 15260.
Received March 13, 1992

Abstract: The thermally equilibrated (298 ± 3 K) gas-phase ion-molecule reactions of trimethyl phosphate with a variety of anions in 0.3 Torr of helium buffer gas have been examined using the flowing afterglow technique. Inorganic anions including amide, hydroxide, alkoxides, and fluoride, as well as the hydrogen sulfide anion, and organic anions including benzenide, allyl, and benzyl anions, as well as the conjugate bases of acetonitrile and acetaldehyde, were used as reactant anions. Two reaction pathways account for essentially all observations: (i) reductive elimination across a carbon-oxygen bond yielding, as the product ion, $(CH_3O)_2PO^-$ and (ii) nucleophilic substitution at carbon yielding, as the product ion, $(CH_3O)_2PO_2^-$. For all anions that displayed bimolecular reaction pathways, products arising from substitution at carbon are found. The strongest bases (e.g., amide and hydroxide) produce reductive elimination products from trimethyl phosphate. In stark contrast to the reactivity of trimethyl phosphate in solution, particularly in water, anion reaction at phosphorus is completely unimportant, being found as a trace product for the oxygen-centered nucleophiles only. The reaction at phosphorus, an S_N2-type process, cannot compete with the S_N2 reaction at carbon, because the reaction at carbon has a better leaving group. The bracketed gas-phase acidity of dimethyl phosphate is found to be $\Delta H°_{acid}[(CH_3O)_2PO_2H]$ = 332 ± 4 kcal mol^{-1}.

Phosphate esters are an integral part of many biologically active molecules ranging from DNA and ATP to pesticides and nerve agents.[1] It follows then that reactions of phosphate esters, typically called phosphate-transfer reactions, play a critical role in the chemical processes of life. The mechanism by which enzyme-catalyzed phosphate transfers occur has been studied extensively using both enzymatic and model systems in the condensed phase[2,3] and theoretical modeling in the gas phase;[4] enzymatic

[†] Harvard University.
[‡] University of Pittsburgh.

(1) Emsley, J.; Hall, D. *The Chemistry of Phosphorus*; John Wiley: New York, 1976; Chapters 11 and 12.

0002-7863/92/1514-8619$03.00/0

systems are generally believed to proceed mainly via cleavage of the P–O bond.

The factors that control the reactions of trimethyl phosphate (I) have been studied extensively as a model system for enzymatic reactions. For example, Oberhammer[5] and Van Wazer and Ewig[6]

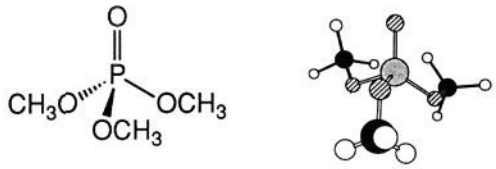

I

have studied the structure of trimethyl phosphate (I) by vapor-phase electron diffraction and ab initio calculations, respectively. The three-dimensional structure of trimethyl phosphate depicted here is a composite of the lowest energy conformation obtained from ab initio calculations and the bond angles and bond lengths found by electron diffraction. This representation is a composite because Oberhammer assumed that trimethyl phosphate had C_3 symmetry in order to solve the structure; however, Van Wazer and Ewig calculated that the lowest energy conformation was completely asymmetric.

In the condensed phase, the reactions of a wide variety of nucleophiles with trimethyl phosphate have been examined in detail. Small nucleophiles such as hydroxide,[7,8] alkoxides,[9] enolates,[10] thiolates,[11] phenyl lithiums,[12] and phenyl grignards[13] yield products arising from nucleophilic attack at phosphorus, while bulky nucleophiles such as bromide,[14] iodide,[14] benzyl lithium,[15] trityl magnesium chloride,[15] and *tert*-butyl amine[16] yield products arising from nucleophilic attack at carbon. As one specific example, Westheimer and co-workers[17] studied the fate of trimethyl phosphate under aqueous alkaline conditions and found that it hydrolyzes to dimethyl phosphate at a rate ($k_{obs} = 3.4 \times 10^{-4}$ M^{-1} s^{-1}) that is 2×10^5 times faster than the rate of hydrolysis of the dimethyl phosphate anion to methyl phosphate dianion. In a related study, Westheimer and co-workers[18] found that, under aqueous alkaline conditions, trimethyl phosphite hydrolyzes 600 times faster than does trimethyl phosphate.

Several aspects of the reactivity of trimethyl phosphate have been briefly examined in the gas phase. Asubiojo and co-workers[19] measured the rate of appearance of methoxide from the reaction of trimethyl phosphate with hydroxide using the ion cyclotron resonance (ICR) technique and reported $k_{obs} = 3.2 \times 10^{-10}$ cm^3 $molecule^{-1}$ s^{-1}, while Filley[20] briefly examined its reactions with amide and hydroxide using the flowing afterglow technique; the preliminary data from this latter study suggest that these two reactant anions preferentially react at carbon by nucleophilic substitution. Hodges and co-workers[21] have studied the reactions of several inorganic anions with trimethyl phosphate using the ICR technique. They found mainly nucleophilic substitution at carbon; however, their reported yields for *reaction at carbon* are only upper limits.

In the gas-phase studies reported to date, all the nucleophiles surveyed have similar structures; i.e., they are all localized heteroatomic bases. All of them are reported to react predominantly but not exclusively by nucleophilic substitution at carbon. In order to favor reaction at phosphorus, we hypothesized that one needs a charge-delocalized nucleophile on the basis of two pieces of information. First, in the liquid phase, an anionic, heteroatomic, localized nucleophile like hydroxide will be extensively solvated and will have its charge delocalized to some extent by these solvent interactions. Thus, the structure and reactivity properties of hydroxide in liquid solution (where it attacks the phosphorus of trimethyl phosphate) are considerably different than in the gas phase (where the preliminary experiments noted above indicate substitution at carbon occurs). These differences show up in the relative basicity of hydroxide in the two phases.[22] Second, allyl anion, of identical basicity to hydroxide in the gas phase, but of considerable delocalized nature and in mimicking, to some extent, the "softer" identity of completely hydrated hydroxide, displays unique reactivity with dimethyl sulfite.[23] Because these delocalized carbon anions react mostly at sulfur while the heteroatomic bases react mostly at carbon in the dimethyl sulfite case, we hypothesized that these same delocalized anions would be the gas-phase anions that would have the greatest propensity to react at phosphorus in their reactions with trimethyl phosphate.

In addition to the specific reasons described above, we chose to use room temperature conditions readily obtained with the flowing afterglow to study the organic dynamics of trimethyl phosphate as part of our interest in the intrinsic reactivity of anions with prototypical organic esters such as methyl acetate,[24] methyl pyruvate,[25] and dimethyl sulfite[23] and related molecules such as dimethyl disulfide.[26] In this work, we report the reaction rates, the products observed, and our mechanistic interpretations of the reactions of trimethyl phosphate with a diverse set of anions (both in structure and basicity) in the gas phase. We are interested in the factors that control the site of reactivity (C or P) and the specific type of reaction that occurs at each center. These studies focus on the intramolecular competitive chemical processes that result when a bare anion (in the absence of any counter ion, any solvent molecules, or any type of aggregation) encounters a single trimethyl phosphate molecule.

Experimental Section

These experiments were carried out at ambient temperature (298 ± 3 K) and in 0.3 Torr of helium buffer gas in a flowing afterglow[27,28] which has been previously described.[29] Amide, the atomic oxygen anion, and methoxide were generated by dissociative electron attachment to

(2) Frey, P. A. *Tetrahedron* **1982**, *38*, 1541–1567. Benkovic, S. J.; Schray, K. J. In *The Enzymes*, 3rd ed.; Boyer, P., Ed.; Academic Press: New York, 1973; Vol. 8, Chapter 6.

(3) Westheimer, F. H. *Chem. Rev.* **1981**, *81*, 313–326.

(4) Lim, C.; Karplus, M. *J. Am. Chem. Soc.* **1990**, *112*, 5872–5873. Dejaegere, A.; Lim, C.; Karplus, M. *J. Am. Chem. Soc.* **1991**, *113*, 4353–4355.

(5) Oberhammer, H. *Z. Naturforsch.* **1973**, *28A*, 1140–1144.

(6) Van Wazer, J. R.; Ewig, C. S. *J. Am. Chem. Soc.* **1986**, *108*, 4354–4360.

(7) Blumenthal, E.; Herbert, J. B. M. *Trans. Faraday Soc.* **1945**, *41*, 611–617.

(8) Barnard, P. W. C.; Bunton, C. A.; Llewellyn, D. R.; Vernon, C. A.; Welch, V. A. *J. Chem. Soc.* **1961**, 2670–2676.

(9) Cox, J. R.; Ramsay, O. B. *Chem. Rev.* **1964**, *64*, 317–352. Bunton, C. A. *Acc. Chem. Res.* **1970**, *3*, 257–265.

(10) Gompper, R.; Vogt, H. H. *Chem. Ber.* **1981**, *114*, 2866–2883.

(11) Savignac, P.; Coutrot, P. *Synthesis* **1974**, *11*, 818–819.

(12) Willans, J. L. *Chem. Ind. (London)* **1957**, 235–236.

(13) Dawson, N. D.; Burger, A. *J. Org. Chem.* **1953**, *18*, 207–210.

(14) Hudson, R. F.; Harper, D. C. *J. Chem. Soc.* **1958**, 1356–1360.

(15) Gilman, H.; Gaj, B. J. *J. Am. Chem. Soc.* **1960**, *82*, 6326–6329.

(16) Dostrovsky, I.; Halmann, M. *J. Chem. Soc.* **1953**, 511–516. Gray, M. D. M.; Smith, D. J. H. *Tetrahedron Lett.* **1980**, *21*, 859–860.

(17) Westheimer, F. H. *Science* **1987**, *235*, 1173–1178. Kumamoto, J.; Cox, J. R.; Westheimer, F. H. *J. Am. Chem. Soc.* **1956**, *78*, 4858–4860. Kumamoto, J.; Westheimer, F. H. *J. Am. Chem. Soc.* **1955**, *77*, 2515–2518.

(18) Westheimer, F. H.; Hwang, S.; Covitz, F. *J. Am. Chem. Soc.* **1988**, *110*, 181–185.

(19) Asubiojo, O. I.; Brauman, J. I.; Levin, R. H. *J. Am. Chem. Soc.* **1977**, *99*, 7707–7708.

(20) Filley, J. Ph.D. Thesis, University of Colorado, Boulder, 1985.

(21) Hodges, R. V.; Sullivan, S. A.; Beauchamp, J. L. *J. Am. Chem. Soc.* **1980**, *102*, 935–938.

(22) $pK_a[H_2O] = 15.7$ and $pK_a[CH_3OH] = 16$ while $\Delta H°_{acid}[H_2O] = 390.8$ kcal mol^{-1} and $\Delta H°_{acid}[CH_3OH] = 381.7$ kcal mol^{-1}. Lowry, T. H.; Richardson, K. S. *Mechanism and Theory in Organic Chemistry*, 3rd ed.; Harper & Row: New York, 1987; pp 300–301.

(23) Grabowski, J. J.; Lum, R. C. *J. Am. Chem. Soc.* **1990**, *112*, 607–620.

(24) Grabowski, J. J.; Pohl, N.; Lum, R. C. Unpublished results.

(25) Grabowski, J. J.; Goroff, N. S. Unpublished results.

(26) Grabowski, J. J.; Zhang, L. *J. Am. Chem. Soc.* **1989**, *111*, 1193–1203.

(27) Ferguson, E. E.; Fehsenfeld, F. C.; Schmeltekopf, A. L. In *Advances in Atomic and Molecular Physics*; Bates, D. R., Estermann, I., Eds.; Academic Press: New York, 1969; Vol. 5, pp 1–56.

(28) Graul, S. T.; Squires, R. R. *Mass Spectrom. Rev.* **1988**, *7*, 263–358.

(29) Grabowski, J. J.; Melly, S. J. *Int. J. Mass Spectrom. Ion Processes* **1987**, *81*, 147–164.

ammonia, nitrous oxide, and methanol, respectively. Hydroxide was generated by allowing the atomic oxygen anion to abstract a hydrogen atom from methane.[30] HS^- was formed by allowing HO^- to react with carbon disulfide.[31] All other reactant anions were produced by exothermic proton transfers from an appropriate neutral to amide anion (e.g., $CH_3CH_2CH_2NH^-$ from $CH_3CH_2CH_2NH_2$).

Trimethyl phosphate, $(CH_3O)_3PO$, (Aldrich Gold Label, 99+%) was used as received. The ^1H and ^{31}P NMR spectra of trimethyl phosphate in $CDCl_3$ revealed no impurities. GC analysis of trimethyl phosphate indicated that the sample was >99% pure; no impurities were observed. Propyl amine was distilled before use. All other reagents were obtained from standard commercial sources and were used as received. Before use, each liquid sample was subjected to several freeze–pump–thaw cycles to remove dissolved gases.

Because trimethyl phosphate is a relatively nonvolatile liquid (bp (760 mm) 197 °C),[32] for many of these experiments, but not all, a low flow of sweep gas (helium or argon) was gently bubbled through the trimethyl phosphate and used to carry the phosphate into the flow tube at higher flow rates than can be achieved by the normal direct distillation method. The ^1H NMR spectrum of trimethyl phosphate after it had been used with the "bubbler" and positive ion chemical ionization of the same sample of trimethyl phosphate in the flowing afterglow using CH_5^+/$C_2H_5^+$, gave no indication that trimethyl phosphate underwent decomposition either in the "bubbler" or in the vapor phase when added to the flow tube in this manner.

Reactions of interest were examined in several different ways: by qualitative experiments to identify all reaction products, by kinetic experiments to measure total reaction rate coefficients, and by branching-ratio experiments to quantitate the yields of the various product ions. The qualitative experiments entailed taking a complete mass scan of the ionic contents of the flow tube at each of several times during the course of a reaction.

The rate coefficient for amide reacting with trimethyl phosphate was determined by quantitatively monitoring the decrease in amide signal as a function of distance (time) at a constant trimethyl phosphate concentration under pseudo-first-order conditions, as previously described.[33] Higher trimethyl phosphate flows, needed to attain adequate reactant ion falloff, were achieved by using the bubbler system described above; this procedure necessitated that we measure most rate coefficients relative to that for amide. The decrease in the reactant ion signal (produced via the appropriate proton transfer with amide) as a function of distance (time) was measured in the standard way. Without changing the flow or the pressure of helium in the flow tube or the flow of the sweep gas through the trimethyl phosphate, delivery of the reactant ion precursor gas was stopped so that amide became the reactant ion. The decrease in the amide ion signal as a function of distance was followed in a manner identical to that for the reactant ion of interest. Since the *only* difference between these two observed semilog decay plots is the identity of the reactant ion, the absolute rate coefficient for the reactant ion of interest was obtained by taking the ratio of the slopes of the plots and multiplying by the independently determined absolute rate coefficient for the amide reaction.

Collisional rate coefficients (k_{coll}) were calculated according to the variational transition-state trajectory theory of Su and Chesnavich,[34] using a dipole moment[35] for trimethyl phosphate of 3.19 D and a polarizability of 1.15×10^{-23} cm^3 obtained as the average of values calculated from the index of refraction[36] and group additivity.[37] Reaction efficiencies are determined as the ratio of the observed rate coefficient to that of the collisional rate coefficient (EFF = k_{obs}/k_{coll}).

Quantitative measurements of the branching ratios (i.e., the primary product distributions) were made by monitoring the reactant and product ions at a fixed concentration of neutral reagent (pseudo-first-order reaction conditions) and following the reaction as a function of distance (time) in a manner analogous to that used for the kinetics measurements, as previously described.[23,26] When we measure branching ratios, we monitor only the most intense isotopic peak for each ion. However, because of the existence of natural isotopes, we may "miss" different proportions of the true chemical yield of each ion. We correct for this fact by dividing the observed ion yield by the necessary correction factor computed from standard isotope tables;[38] these isotope factors are included in Table I.

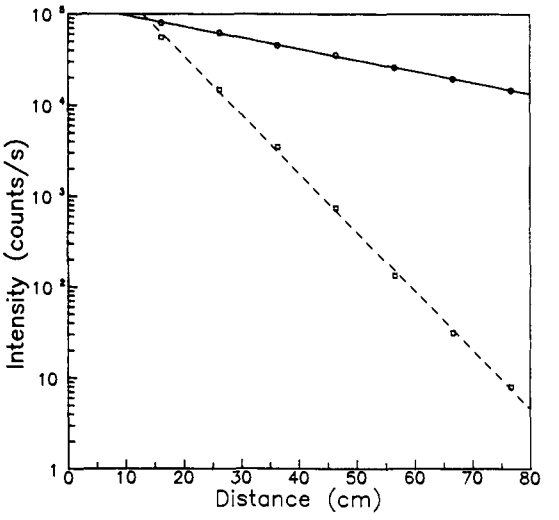

Figure 1. Semilog plot of the observed allyl anion intensity (—) and amide intensity (---) as a function of distance (time) at a constant concentration of trimethyl phosphate. For the one independent determination shown, the absolute rate coefficient for the allyl anion reaction, obtained as the ratio of the allyl anion slope (R = 0.9997, error in slope = 1.0%) to the amide slope (R = 0.9994, error in slope = 1.4%) multiplied by the absolute amide rate coefficient, is 6.78×10^{-10} cm^3 molecule^{-1} s^{-1}. In this example, the allyl anion reaction was followed for 2.5 half-lives and the amide ion reaction for 12.8 half-lives.

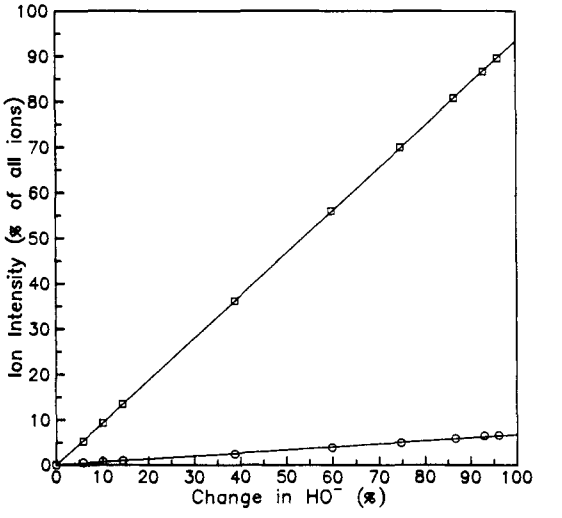

Figure 2. Branching-ratio plot for the reaction of hydroxide with trimethyl phosphate at 0.3 Torr of helium and 298 K. The lines are those defined by eq 2 in ref 23, the slopes of which yield the "observed amounts" of the two product ions: 6.7% m/z 109 (○) and 93.3% m/z 125 (□) for one determination.

Results

The rate coefficients and the branching ratios obtained for the thermally-equilibrated (298 K) reactions of anions with trimethyl

(30) Bohme, D. K.; Fehsenfeld, F. C. *Can. J. Chem.* **1969**, *47*, 2717–2719.
(31) Bierbaum, V. M.; Grabowski, J. J.; DePuy, C. H. *J. Phys. Chem.* **1984**, *88*, 1389–1393.
(32) *Handbook of Chemistry and Physics*, 71st ed.; Lide, D. R., Ed.; CRC Press: Boston, MA, 1990; p 6–56.
(33) Guo, Y.; Grabowski, J. J. *J. Am. Chem. Soc.* **1991**, *113*, 5923–5931.
(34) Su, T.; Chesnavich, W. J. *J. Chem. Phys.* **1982**, *76*, 5183–5185.
(35) Waeschke, H.; Mitzner, R. *Z. Chem.* **1979**, *19*, 379–380.
(36) Using η = 1.3960 in the Lorentz–Lorenz relation cited in: Shoemaker, D. P.; Garland, W. C.; Steinfeld, J. I.; Nibler, J. W. *Experiments in Physical Chemistry*, 4th ed.; McGraw Hill: New York, 1981; p 383.
(37) Miller, K. J.; Savchik, J. A. *J. Am. Chem. Soc.* **1979**, *101*, 7206–7213.
(38) de Bievre, P.; Barnes, I. L. *Int. J. Mass Spectrom. Ion Processes* **1985**, *65*, 211–230.
(39) Lias, S. G.; Bartmess, J. E.; Liebman, J. F.; Holmes, J. L.; Levin, R. D.; Mallard, W. G. *J. Phys. Chem. Ref. Data* **1988**, *17*, Suppl. No. 1. This data, in a slightly updated form is also available to us on a personal computer by way of: NIST Negative Ion Energetics Database (Version 2.06, January 1990), NIST Standard Reference Database 19B.
(40) Barlow, S. E.; Dang, T. T.; Bierbaum, V. M. *J. Am. Chem. Soc.* **1990**, *112*, 6832–6838.
(41) Ervin, K. M.; Gronert, S.; Barlow, S. E.; Gilles, M. K.; Harrison, A. G.; Bierbaum, V. M.; DePuy, C. H.; Lineberger, W. C.; Ellison, G. B. *J. Am. Chem. Soc.* **1990**, *112*, 5750–5759.

Table I. Results for the Reactions of Anions with Trimethyl Phosphate in the Gas Phase at 298 K

anion (A^-)	$\Delta H°_{acid}$(AH) (kcal mol^{-1})[a]	prod ion (m/z)	obs amt[b]	n_{BR}[c]	mol form.	prod yield (%)[d]	$k_{tot} \pm 1\sigma$[e]	EFF[f]	n_k[c]
H_2N^-	403.7	109	0.593 ± 0.013	4	$(C_2H_6O_3P)^-$	59.3	3.56 ± 0.57	0.79	5
		125	0.407 ± 0.013		$(C_2H_6O_4P)^-$	40.7			
$C_6H_5^-$	400.8	109	0.080 ± 0.016	2	$(C_2H_6O_3P)^-$	7.9	1.52 ± 0.32	0.62	5
		125	0.920 ± 0.016		$(C_2H_6O_4P)^-$	92.1			
$CH_3CH_2CH_2NH^-$	398.4	109	0.530 ± 0.012	3	$(C_2H_6O_3P)^-$	52.9	2.22 ± 0.49	0.82	5
		125	0.470 ± 0.012		$(C_2H_6O_4P)^-$	47.1			
HO^-	390.8	109	0.069 ± 0.003	2	$(C_2H_6O_3P)^-$	6.9	3.10 ± 0.10	0.71	4
		125	0.931 ± 0.003		$(C_2H_6O_4P)^-$	93.1			
$H_2C{=}CHCH_2^-$	390.8	125	1.00		$(C_2H_6O_4P)^-$	100	0.658 ± 0.05	0.21	5
CD_3O^-	382.1[g]	125	0.985 ± 0.001	2	$(C_2H_6O_4P)^-$	98.5			
		128	0.015 ± 0.002		$(C_2D_3H_3O_4P)^-$	1.5			
CH_3O^-	381.7[h]	125	1.00		$(C_2H_6O_4P)^-$	100	1.90 ± 0.55	0.58	5
$C_6H_5CH_2^-$	380.7	125	1.00		$(C_2H_6O_4P)^-$	100			
$CH_3CH_2O^-$	377.4	125	0.989 ± 0.001	2	$(C_2H_6O_4P)^-$	98.9	1.81 ± 0.17	0.61	5
		139	0.011 ± 0.001		$(C_3H_8O_4P)^-$	1.1			
HCC^-	376.7	125	1.00		$(C_2H_6O_4P)^-$	100			
$(CH_3)_3CO^-$	374.6	125	1.00		$(C_2H_6O_4P)^-$	100	1.34 ± 0.09	0.53	5
$H_3COCH_2CH_2O^-$	373.8	125	1.00		$(C_2H_6O_4P)^-$	100			
H_2CCN^-	372.8	125	1.00		$(C_2H_6O_4P)^-$	100	≤0.14	≤0.05	4
F^-	371.3	125	1.00		$(C_2H_6O_4P)^-$	100			
$H_2C{=}C(H)O^-$	365.9	125	1.00		$(C_2H_6O_4P)^-$	100			
HS^-	351.1	125	1.00		$(C_2H_6O_4P)^-$	100	0.084 ± 0.01	0.02	5
Cl^-	333.7	175	1.00		$(C_2H_9ClO_4P)^-$	100			

[a] See ref 39 for source of gas-phase acidities. [b] The average fractional yield ± one standard deviation based on observation of only the m/z values listed for that reaction. These observed yields for the reactions of amide, phenide, and propyl amide have been corrected to remove any contributions from the reaction of a hydroxide impurity with trimethyl phosphate. [c] The number of independent experimental determinations of the branching ratio (BR) or rate coefficient (k). [d] The yield of the product ion of the given molecular formula actually found in the reaction cited (i.e., corrected to include all naturally occurring isotopic variants). The product yields are calculated by taking the "obs amt" and dividing it by the "isotope factor" and then renormalizing. The isotope factor is the fraction of the product ion with the given molecular formula that will be detected at the m/z value listed (which is the predominant isotopic peak). These factors were calculated from values in the Table of the Isotopes in ref 38. The isotope factors for m/z 109, 125, 128, 139, and 175 are 0.9703, 0.9680, 0.9684, 0.9570, and 0.7250, respectively. [e] Reaction rate in units of 10^{-9} cm^3 molecule^{-1} s^{-1}. [f] Reaction efficiency, k_{obs}/k_{coll}, where k_{coll} is calculated according to ref 34. [g] Reference 40. [h] Reference 41.

phosphate in 0.3 Torr of helium are collected in Table I. An example of one of the independent experiments used to determine the relative rate coefficient for the allyl anion plus trimethyl phosphate reaction is shown in Figure 1. The observed precision of the measured amide rate coefficient is ±16% (one standard deviation of the sample), while we estimate the absolute accuracy as ±20%. The main contribution to the absolute error is our inability to measure pressure accurately; our repetitive measurements are designed with this limitation in mind, to provide the most accurate estimate of the true rate coefficient at some sacrifice in precision. The relative rate coefficients have only a slightly larger error than those determined in the standard way; the average percent difference in the slopes was 3% (determined from a linear least squares fit), for the relative rate in which amide was both the reactant and the precursor ion.

A small amount of hydroxide (from "adventitious water") is often found in the reactant ion spectra for bases stronger than hydroxide. We always correct our observed branching ratios for those reactant ions more basic than HO^- to remove contributions due to the reactions of the contaminating hydroxide signal. This correction was done on a point by point basis as previously described.[23,42] The precision of our branching-ratio measurements is shown in Table I, while we estimate that the error in the accuracy of our measurements is a few percent or less.[23] A representative branching-ratio plot for the reaction of hydroxide with trimethyl phosphate is shown in Figure 2. Representative branching-ratio plots for the reactions of amide, benzenide, propyl amide, and methoxide with trimethyl phosphate can be found in the supplementary material. Examination of these plots shows that the product ion yields track linearly with the extent of the reaction, indicating that there are no fast secondary reactions occurring between these first-formed product ions and a second equivalent of trimethyl phosphate.

In order to bracket the acidity of dimethyl phosphate between Brönsted acids of known strength (eq 1), we have examined the reactions of m/z 125, $(CH_3O)_2PO_2^-$ (produced via the reaction

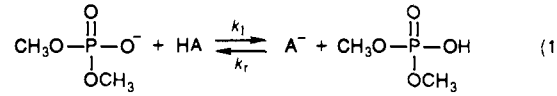

(1)

of HO^- with $(CH_3O)_3PO$), with a series of well characterized acids; these results are collected in the supplementary material. In order to strengthen our determination of the acidity of $(CH_3O)_2PO_2H$, we wished to examine the process defined by k_r of eq 1 as well; however, dimethyl phosphate, available as one component in a mixture,[43] was too nonvolatile for introduction into the flow tube even with use of the "bubbler".

Discussion

The acidity-bracketing study of dimethyl phosphate, $(CH_3O)_2PO_2H$ (supplementary material), indicates that $(CH_3O)_2PO_2^-$ will readily abstract a proton from Cl_2CHCO_2H and CF_3CO_2H but not from HCl or any weaker acid. With HCl and all weaker acids, $(CH_3O)_2PO_2^-$ either reacts slowly (relative to Cl_2CHCO_2H and CF_3CO_2H) to yield the cluster ion or does not react at all. Exothermic proton transfers involving bases with heteroatoms at the basic site are generally found to be fast, while cluster or adduct ion formation is usually slowed under our reaction conditions due to termolecular nature of this latter reaction channel.[44] We believe that the lack of proton transfer between $(CH_3O)_2PO_2^-$ and a Brönsted acid is indicative of a thermochemical barrier. Therefore, we bracket the acidity of $(CH_3O)_2PO_2H$ between Cl_2CHCO_2H ($\Delta G°_{acid}$ = 321.9 ± 2.0 kcal mol^{-1}) and HCl ($\Delta G°_{acid}$ = 328.0

(42) When the competing hydroxide reaction is ignored, the branching ratio obtained for the reaction of amide (average of four measurements) yielded 54.7 ± 1.3% m/z 109 and 45.3 ± 1.2% m/z 125. Comparison of this "uncorrected" branching ratio to the best value which is listed in Table I for the amide–trimethyl phosphate reaction shows that the overall correction is small, but none the less significant.

(43) Dimethyl phosphate (Pfaltz and Bauer) was a mixture of dimethyl phosphate (41–44%), monomethyl phosphate (50–53%), phosphoric acid (0.01–8%), and methanol (0.01–1%) by weight.

(44) Ikezoe, Y.; Matsuoka, S.; Takebe, M.; Viggiano, A. *Gas Phase Ion-Molecule Reaction Rate Constants through 1986*; Maruzen Company: Japan, 1987.

Scheme I. Generalized Scheme for the Reactions of Anions with Trimethyl Phosphate at 298 K

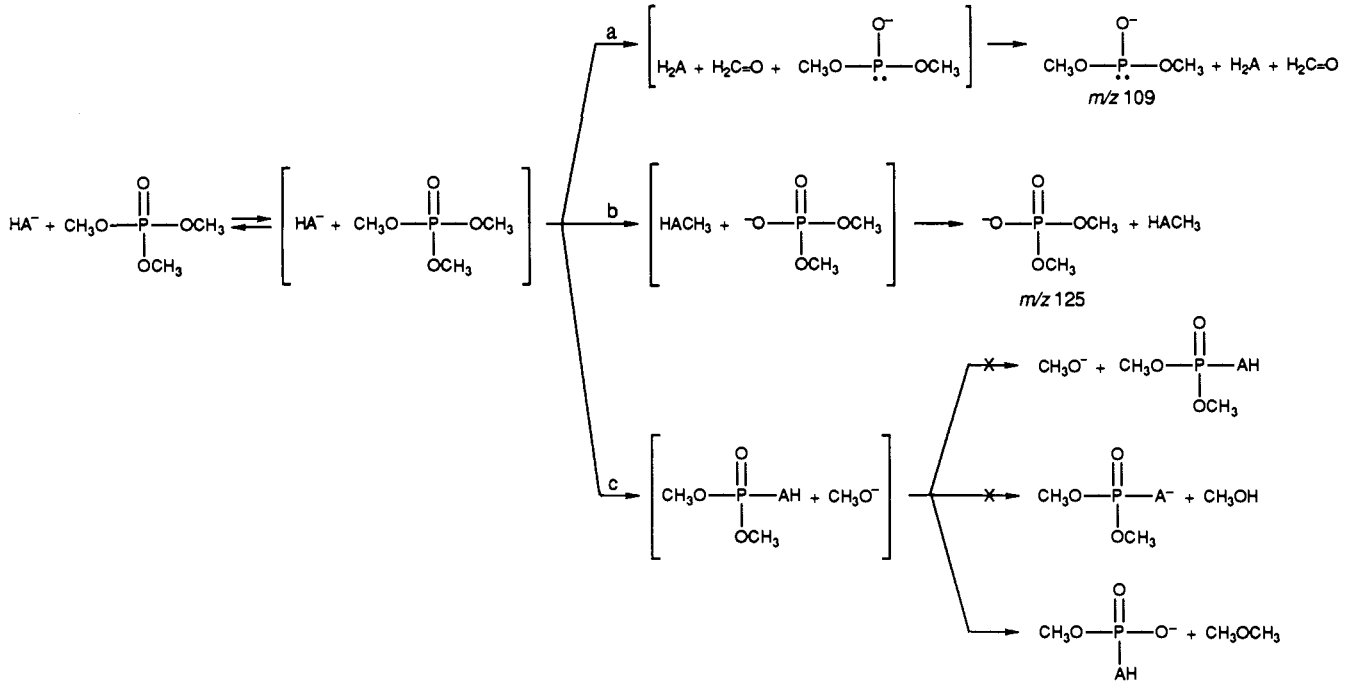

± 0.3 kcal mol^{-1}) and assign $\Delta G°_{acid}[(CH_3O)_2PO_2H] = 325 \pm 4$ kcal mol^{-1}. Using[45] $\Delta S°_{acid}[(CH_3O)_2PO_2H] = 23.1$ cal mol^{-1} K^{-1}, we define $\Delta H°_{acid}[(CH_3O)_2PO_2H] = 332 \pm 4$ kcal mol^{-1}. The relatively large error bars on the bracketed acidity of dimethyl phosphate are due to several factors: (i) the error bars associated with the acidity values of the reference acids; (ii) the slight ambiguity introduced by the slow association reactions; and (iii) the limitation of being forced to examine eq 1 in only one direction.[46] The relative gas-phase acidities of CF_3CO_2H and $(CH_3O)_2PO_2H$ therefore mimic their aqueous values: $pK_a[(CH_3O)_2PO_2H] = 0.76$ and $pK_a[CF_3CO_2H] = 0.52$.[47,48]

We can obtain the heat of formation of the dimethyl phosphate anion using our measured acidity and the definition of the acidity of dimethyl phosphate (eq 2). Using eq 2b and $\Delta H°_{acid}$-

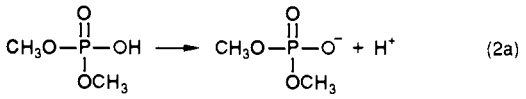

(2a)

$$\Delta H°_{acid}[(CH_3O)_2PO_2H] = \Delta H°_f[(CH_3O)_2PO_2^-] + \Delta H°_f[H^+] - \Delta H°_f[(CH_3O)_2PO_2H] \quad (2b)$$

$[(CH_3O)_2PO_2H] = 332 \pm 4$ kcal mol^{-1}, $\Delta H°_f[H^+] = 365.7$ kcal mol^{-1}, and $\Delta H°_{f\,est}[(CH_3O)_2PO_2H] \approx -271 \pm 3$ kcal mol^{-1} (from group additivity),[49,50] we derive $\Delta H°_f[(CH_3O)_2PO_2] = -305 \pm 4$ kcal mol^{-1}. This heat of formation of the dimethyl phosphate anion will be needed in our analysis of the thermochemistry of the reaction paths found (or not found) for anions with trimethyl phosphate.

Table II. Product Channels and Enthalpies for the Reaction of Anions with Trimethyl Phosphate at 298 K

anion	$\Delta H°_{acid}$[HA] (kcal mol^{-1})[a]	yield (%)		$\Delta H°_{rxn}$ (kcal mol^{-1})[b]	
		$E_{CO}2$	S_N2	$E_{CO}2$[c]	S_N2
H_2N^-	403.7	59	41	−14	−81
$C_6H_5^-$	400.7	8	92	−11	−91
$CH_3CH_2CH_2NH^-$	398.4	52	48	−9	−80
HO^-	390.8	7	93	−1	−64
$H_2C{=}CHCH_2^-$	390.8		100	−1	−78
CD_3O^-	382.1[d]		99[f]	8	−59
CH_3O^-	381.7[e]		100	9	−59
$PhCH_2^-$	380.7		100	9	−68
$CH_3CH_2O^-$	377.4		99[f]	13	−55
HCC^-	376.7		100	13	−69
$(CH_3)_3CO^-$	374.6		100	15	−50
$H_3COCH_2CH_2O^-$	373.8		100	17	−50
H_2CCN^-	372.8		100	17	−61
F^-	371.8		100	19	−48
$H_2C{=}C(H)O^-$	365.9		100	24	−53
HS^-	351.1		100	39	−34

[a] All acidities are taken from ref 39. [b] The heats of reaction are estimated using values from ref 39, $\Delta H°_f[(CH_3O)_3PO] = -257$ kcal mol^{-1} from group additivity[49] and $\Delta H°_f[(CH_3O)_2PO_2^-] = -305$ kcal mol^{-1} (see text). The error in these reaction enthalpies is ±4 kcal mol^{-1}. [c] The Gibbs free energy of this reactant channel will be more exoergic than the enthalpic values listed here due to the increase in the number of the particles as the reaction proceeds. For instance, $\Delta G°_{rxn}$ for HO^-, giving $E_{CO}2$ products, is approximately −7 kcal mol^{-1}. [d] Reference 40. [e] Reference 41. [f] The reactions of CD_3O^- and $CH_3CH_2O^-$ also yield 1% products arising from attack at phosphorus.

(45) Bartmess, J. E.; McIver, R. T., Jr. In *Gas Phase Ion Chemistry*; Bowers, M. T., Ed.; Academic Press: New York, 1979, Vol. 2, Chapter 11. The estimate assumes that there is no contribution to the entropy of ionization from translational, vibrational, or electronic considerations, while the loss of the OH rotor and external rotations contributes −2.9 eu.

(46) Numerous examples appear in the published literature in which Brönsted acidities are evaluated by bracketing reactions carried out in one direction only; representative citations include: (a) benzyne radical anion,[33] (b) thiomethyl anion (Kass, S. R.; Guo, H.; Dahlke, G. D. *J. Am. Soc. Mass Spectrom.* **1990**, *1*, 366–371), (c) silaacetylide anion (Damrauer, R.; DePuy, C. H.; Barlow, S. E.; Gronert, S. *J. Am. Chem. Soc.* **1988**, *110*, 2005–2006), and (d) immonium ion (Peerboom, R. A. L.; Ingemann, S.; Nibbering, N. M. M.; Liebman, J. F. *J. Chem. Soc., Perkin Trans. 2* **1990**, 1825–1828).

(47) Bunton, C. A.; Mhala, M. M.; Oldham, K. G.; Vernon, C. A. *J. Chem. Soc.* **1960**, 3293–3301.

(48) *Ionisation Constants of Organic Acids in Aqueous Solution*; Sergeant, E. P., Dempsey, B., Eds.; Pergamon Press: New York, 1979.

(49) Benson, S. W. *Thermochemical Kinetics*, 2nd ed.; Wiley & Sons: New York, 1976.

(50) The heats of formation for phosphates estimated by group additivity are in excellent agreement with the experimentally determined values. For example, for triethyl phosphate $\Delta H°_{f\,est}[(CH_3CH_2O)_3PO] \approx -282$ kcal mol^{-1} while $\Delta H°_{f\,exp}[(CH_3CH_2O)_3PO] = -283.6$ kcal mol^{-1}, and for tripropyl phosphate $\Delta H°_{f\,est}[(CH_3CH_2CH_2O)_3PO] \approx -296$ kcal mol^{-1} while $\Delta H°_{f\,exp}$-$[(CH_3CH_2CH_2O)_3PO] = -300.5$ kcal mol^{-1}. The experimental heats of formation are taken from: Pedley, J. B.; Rylance, J. *Sussex*-N.P. L. *Computer Analyzed Thermochemical Data: Organic and Organometallic Compounds*; University of Sussex: Sussex, England, 1977. All heats of formation used in this work are included in the supplementary material.

The data in Table I show that most of the reactant anions examined undergo fast reaction with trimethyl phosphate; of the anions whose reaction rates we measured, only the conjugate base of acetonitrile and the hydrogen sulfide anion undergo slow (EFF $\leq$ 0.1) reaction with trimethyl phosphate. We can account for the observed reactions of anions with trimethyl phosphate using a general scheme involving three pathways: elimination across the carbon–oxygen bond, $E_{CO}2$, (Scheme I, path a), nucleophilic substitution at carbon (Scheme I, path b), and reaction at phosphorus (Scheme I, path c). Without exception, for all of the anions that we have examined, products arising from a substitution process at phosphorus account for less than 2% of the observed products and, in most cases, the amounts if formed are below our detection limit of 0.2%. Note that, in Scheme I, the species shown in brackets are the key ion–molecule complexes on the reaction coordinate but are not directly observed in the reactions that yield bimolecular products.

In Table II, we have summarized the data of Table I in terms of the two possible reaction channels and have included estimates of the reaction enthalpies of each channel. Furthermore, we think about the reactant anions listed in Table II as three different types of bases: (i) localized heteroatomic bases (e.g., H_2N^-, HO^-), (ii) localized carbon bases (e.g., $C_6H_5^-$), and (iii) delocalized carbon bases (e.g., $H_2C{=}CHCH_2^-$). We have previously separated reactant anions into these three different classes because of the distinct reactivity each class of anion displays when allowed to react with a variety of organic substrates such as dimethyl disulfide,[26] dimethyl sulfite,[23] and methyl pyruvate,[25] to mention but a few. Since there is essentially no reaction at phosphorus and only reaction at carbon, trimethyl phosphate is an excellent molecule to study competition between nucleophilic substitution and elimination (across a C–O bond) at a common carbon atom.

Elimination reactions across C–O bonds of organic esters have been noted for the reaction of strong bases with dimethyl sulfite,[23] dimethyl carbonate,[51] methyl pyruvate,[25] and dimethyl methylphosphonate.[52] For the trimethyl phosphate, the neutral of interest here, the elimination channel occurs for all localized anions greater than or equal to hydroxide in base strength (Table II); this fragmentation-type reaction produces $(CH_3O)_2PO^- + H_2A + H_2C{=}O$ for a generic base of structure HA^- (Scheme I, path a). The highest yield of elimination was found for the strongest base examined (H_2N^-); as the base strength of the anion falls off, so does the amount of elimination observed. For example, amide gives 59% elimination, while propyl amide, 5.3 kcal mol^{-1} less basic than amide, gives 52% elimination, and hydroxide, 12.9 kcal mol^{-1} weaker than amide, gives only 7% elimination. Benzenide gives just 8% elimination; the relatively low yield of elimination for this strongly carbanion is not unexpected, since localized carbon anions tend to be kinetically slower bases than localized heteroatomic anions of identical base strength. Note that the elimination channel is observed for most cases where it is enthalpically allowed; the one exception is allyl anion. The lack of an elimination channel for allyl anion, while hydroxide, an anion of identical base strength, gives a small amount of $E_{CO}2$ product, is in accord with the generalization that delocalized carbon anions are kinetically poor bases relative to localized heteroatomic anions.[23,53]

For a series of anions, as the base strength decreases, the elimination pathway is reduced in exothermicity and in yield, while the substitution channel remains thermochemically viable and is therefore the exclusive pathway observed for reactant anions less basic than hydroxide. The substitution pathway occurs for *all* anions studied and produces $(CH_3O)_2PO_2^-$ (Scheme I, path b). The consistent high yield of $(CH_3O)_2PO_2^-$ is in accord with the very acidic nature of its conjugate acid, $(CH_3O)_2PO_2H$; therefore, $(CH_3O)_2PO_2^-$ should be considered to be an excellent leaving group for nucleophilic substitution. On the basis of its proton affinity, $(CH_3O)_2PO_2^-$ (PA[$(CH_3O)_2PO_2^-$] = 332 kcal mol^{-1}) might be expected to have a leaving-group ability similar to Cl^- (PA[Cl^-] = 334 kcal mol^{-1}) for S_N2-type processes. When the efficiencies for the reactions of anions with trimethyl phosphate are compared to the efficiencies for the reactions of these same anions with methyl chloride,[54] the trimethyl phosphate reactions are more efficient, suggesting that the dimethyl phosphate anion is a better leaving group than chloride. The prevalence of the substitution pathway is consistent with the observation that, in the gas phase, nucleophilic substitutions generally occur whenever there is both a good leaving group and a substantial driving force.[55]

In addition to reaction at carbon, we observe a trace amount of reaction at phosphorus, when trimethyl phosphate is allowed to react with methoxide-d_3 or ethoxide. The reaction of methoxide-d_3 yields 1.5% $(CD_3O)(CH_3O)PO_2^-$, while the reaction of ethoxide yields 1.1% $(CH_3CH_2O)(CH_3O)PO_2^-$. These products are formed by the reaction of methoxide-d_3 or ethoxide, HA^-, reacting with trimethyl phosphate within an ion–dipole complex to yield methoxide and $(CH_3O)_2POAH$ (Scheme I, path c). The product ion–neutral complex could dissociate in three ways: either methoxide would be observed as a product ion or, much more likely, it would abstract an acidic proton or a methyl group from $(CH_3O)_2POAH$, yielding $(CH_3O)_2POA^-$ or $(CH_3O)(HA)PO_2^-$ as product ions. Because the methoxy-d_3 or ethoxy group on the newly formed phosphate does not possess an acidic hydrogen, the methoxide produced within the product complex reacts again by attacking carbon, yielding $(CH_3O)(HA)PO_2^-$. The amount of phosphorus reaction falls off rapidly as the base strength of the alkoxide decreases; no reaction at phosphorus is detected for either *tert*-butoxide or 2-methoxyethoxide. For all anions that we have studied that react with trimethyl phosphate, absolutely no methoxide is observed; however, Asubiojo and co-workers[19] determined the rate for the production of methoxide from the reaction of hydroxide and trimethyl phosphate. The methoxide observed by Asubiojo and co-workers and Hodges and co-workers[21] may be produced by the reaction of hydroxide with some relatively volatile impurity or from breakdown products from pyrolysis of trimethyl phosphate on hot ionization components of the ICR.[56]

The product distribution for reaction of methoxide-d_3 with trimethyl phosphate shows there are two competitive pathways, reaction at carbon and reaction at phosphorus, but it does not directly reveal the competitive rates for the two channels. The following model is used to determine the relative rates for the two processes. CD_3O^- forms an ion–dipole complex with trimethyl phosphate, in which methoxide-d_3 can either attack carbon, yielding $(CH_3O)_2PO_2^-$, or attack phosphorus, yielding the ion–dipole complex of CH_3O^- and $(CH_3O)_2(CD_3O)PO$. The methoxide within this latter complex reacts as methoxide-d_3 did in the first complex, by attacking carbon or by attacking phosphorus. Substitution at carbon leads to the formation of $(CH_3O)_2PO_2^-$ one third of the time and $(CH_3O)(CD_3O)PO_2^-$ two thirds of the time, while reaction at phosphorus leads to the formation of two ion–dipole complexes: $[CH_3O^- + (CH_3O)_2(CD_3O)PO]$ and $[CD_3O^- + (CH_3O)_3PO]$. These two complexes react in the same manner as they did before. In this model it is assumed that the reaction at phosphorus proceeds via an S_N2-type process (for reasons outlined below) and that the three methoxy groups are equivalent within trimethyl phosphate. A simple computer algorithm is used to determine the true rate of substitution at carbon compared to the rate of substitution at phosphorus. Comparing the experimentally determined product distributions to those calculated by varying the ratio of the rate of substitution at

(51) Grabowski, J. J.; Roy, P. D. Unpublished results.
(52) Grabowski, J. J.; Lum, R. C. Unpublished results.
(53) Farneth, W. E.; Brauman, J. I. *J. Am. Chem. Soc.* **1976**, *98*, 7891–7898.
(54) Experimental rates were taken from ref 44; reaction efficiencies were calculated according to ref 34.
(55) Brauman, J. I.; Olmstead, W. N. *J. Am. Chem. Soc.* **1977**, *99*, 4219–4228. Pellerite, M. J.; Brauman, J. I. *J. Am. Chem. Soc.* **1980**, *102*, 5993–5999. Riveros, J. M.; Jose, S. M.; Takashima, K. In *Advances in Physical Organic Chemistry*; Gold, V., Bethell, D., Eds.; Academic Press: New York, 1985; Vol. 21, pp 197–240. Brauman, J. I.; Dodd, J. A.; Han, C.-C. In *Nucleophilicity*; Harris, J. M., McManus, S. P., Eds.; Advances in Chemistry Series 215; American Chemical Society: Washington, D.C., 1987; Chapter 2.
(56) Caldwell, G.; Bartmess, J. E. *Int. J. Mass Spectrom. Ion Phys.* **1981**, *40*, 269–274.

Scheme II. General Mechanistic Scheme for Possible Reaction Pathways Occurring at Phosphorus for the Gas-Phase Reaction of an Anion with Trimethyl Phosphate[a]

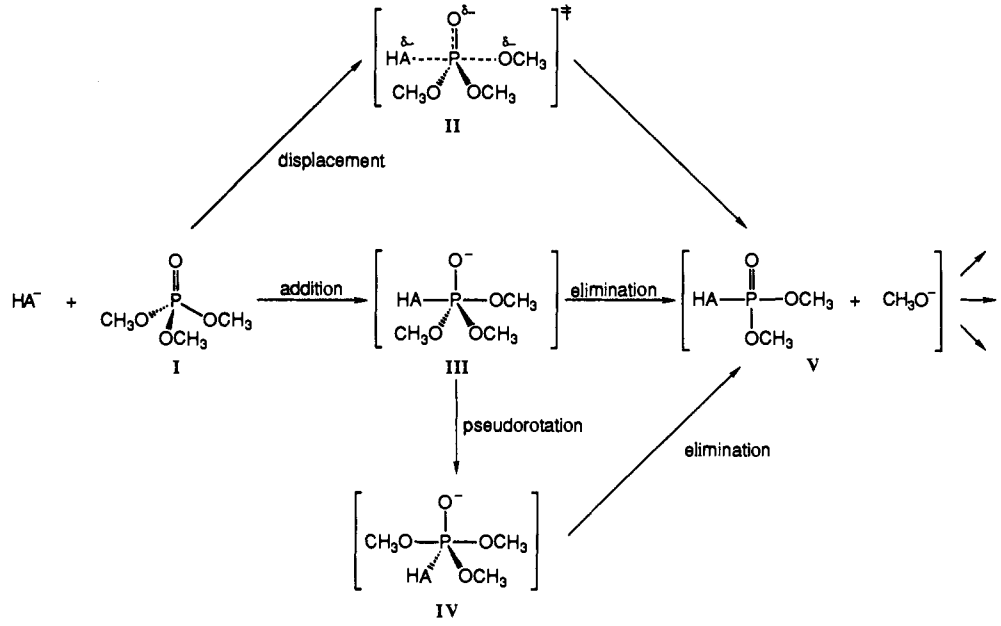

[a] Ion–dipole complexes or intermediates, which would not be observed, are indicated by the brackets. Note that ion–neutral complex V, if ever formed, is expected to have several reactive channels including proton transfer, nucleophilic substitution at carbon, and direct dissociation; hence the arrows from V.

phosphorus to the rate of substitution at carbon leads to the conclusion that the relative rate for reaction at carbon versus reaction at phosphorus is 43:1.

For one of the reactions we examined, that of hydroxide with trimethyl phosphate, we cannot unequivocally distinguish between reaction at the carbon and phosphorus sites, since both reactions are expected to yield the same products. Predominant reaction at carbon with a tiny amount of reaction at phosphorus seems most likely for hydroxide, since amide does not give products arising from attack at phosphorus, while methoxide-d_3 and ethoxide give a small amount (<2%) of products arising from attack at phosphorus; ^{18}O-labeled hydroxide experiments are planned to confirm this expectation.

Why is attack at phosphorus insignificant? Three possible modes for nucleophilic attack at phosphorus have been proposed (Scheme II) on the basis of extensive condensed-phase investigations.[1,2,57] The first is nucleophilic substitution at phosphorus via a pentacoordinate transition structure (II). In this mechanism, the nucleophile attacks at the side opposite the leaving group with simultaneous bond cleavage and bond formation. The transition state II resembles that for bimolecular nucleophilic substitution at saturated carbon; as with the carbon analog, S_N2 reaction at phosphorus will proceed with inversion of configuration at phosphorus.[1,2] The second mechanism, addition–elimination, occurs via formation of a pentacovalent trigonal bipyramidal intermediate (III) followed by the elimination process in a discrete step; groups enter or leave from apical positions. This latter mechanism will also proceed with inversion of configuration at phosphorus.[1,2] The difference between these two mechanisms is the age-old question as to whether there is an intermediate or only a transition state on the reaction coordinate. The process for forming the pentacoordinate transition structure or intermediate is often referred to as "in-line displacement", because the entering and leaving groups are opposite to each other.[58] In the third possible mechanism, the trigonal bipyramidal intermediate formed via addition undergoes pseudorotation,[59] interconverting one trigonal bipyramid (III) to another (IV), as shown in Scheme II. The net result from pseudorotation is that the two apical ligands become equatorial and two equatorial ligands become apical, while the third equatorial ligand remains in an equatorial position.[60] One pseudorotation followed by elimination leads to retention of configuration at phosphorus. This last mechanism is often referred to as the "adjacent" mechanism.[58] For all three mechanisms in the gas phase, methoxide in the product ion–neutral complex V would either be observed as a product ion or react further as described above.

In the condensed phase, addition of a nucleophile to a phosphate to form a pentacoordinate trigonal bipyramidal phosphorane follows "preference rules" that define ligand orientation: (i) groups preferentially enter and leave from the apical position; (ii) electronegative atoms prefer to occupy apical positions; and (iii) π-bonding donor ligands prefer to occupy equatorial positions.[61] For example, if allyl anion were to follow these "preference rules", then it would attack phosphorus, forming a pentacoordinate intermediate in which the allyl group is in the apical position and the O^- is in the equatorial position (III). A phosphorane of such connectivity would prefer to have methoxy groups in both apical positions and the allyl group in an equatorial position, since O is more electronegative than C, and hence the initial pentacoordinate intermediate III would pseudorotate to another (IV). The final pentacoordinate intermediate would then extrude (only) methoxide from the apical position.

We do not observe, however, phosphorus attack for allyl anion nor for most other anions studied. If the pseudorotation mechanism or the addition–elimination mechanism is the preferred mode of phosphorus substitution, there are several reasons why we may not observe phosphorus attack. First, there may be a barrier to pseudorotation so that one may never get to IV, from which loss of only methoxide can occur. Second, if elimination of a leaving group must occur prior to pseudorotation, the adduct III formed from nucleophilic addition to phosphorus may prefer

(57) A fourth possible mechanism involves dissociation of trimethyl phosphate in an S_N1 like fashion, forming CH_3O^- and $CH_3OP(O)(OCH_3)^+$, but such heterolytic bond cleavage at room temperature is energetically prohibited in the gas phase.

(58) Fersht, A. *Enzyme Structure and Mechanism*; W. H. Freeman: New York, 1985; pp 236–237.

(59) Westheimer, F. H. In *Rearrangements in Ground and Excited States*; de Mayo, P., Ed.; Academic Press: New York, 1980; Vol. 2, Essay 10.

(60) Two detailed mechanisms have been proposed for this process. One is the Berry mechanism (Berry, R. S. *J. Chem. Phys.* **1960**, *32*, 933–938) and the other is the turnstile mechanism (Gillespie, P.; Hoffman, P.; Klusacek, H.; Marquarding, D.; Pfohl, S.; Ramirez, F.; Tsolis, E. A.; Ugi, I. *Angew. Chem., Int. Ed. Engl.* **1971**, *10*, 687–715).

(61) Westheimer, F. H. *Acc. Chem. Res.* **1968**, *1*, 70–78.

to break down by cleaving the newly formed phosphorus–nucleophile bond in order to retain the maximum number of phosphorus–oxygen bonds. We believe, however, that the lack of observation of phosphorus substitution products is due to a barrier to addition, rather than a barrier to elimination or pseudorotation. Our preference stems from the observation that methoxide-d_3, when allowed to react with trimethyl phosphate, showed very little deuterium incorporation into the dimethyl phosphate anion product. If a significant amount of addition had occurred, we would have expected to see a statistical scrambling of labeled methoxide into the product.

In the liquid phase, there is little evidence for an addition–elimination mechanism without pseudorotation. Blumenthal and Herbert[7] and Barnard and co-workers[8] demonstrated that, in the reaction of trimethyl phosphate with ^{18}O-labeled hydroxide, one and only one labeled oxygen is incorporated into the product and that exclusive P–O bond cleavage occurs. Their results are consistent with a mechanism for substitution involving a pentacoordinate transition state and not a discrete intermediate. Solvent effects, steric hindrance, inductive effects of the substituents on phosphorus, and product composition in the condensed phase all suggest that an addition–elimination mechanism is not occurring, in accord with our gas-phase data.[62]

In the liquid phase, it has been suggested that nucleophilic reaction at phosphorus takes place via an S_N2-like process.[1,62] If substitution at phosphorus in the gas phase occurs in a similar fashion, then the lack of significant products observed from an S_N2-like process at phosphorus and the facile observation of products from attack at carbon suggest that the barrier for substitution at phosphorus in trimethyl phosphate is higher than that for substitution at carbon. In the liquid phase, high barriers due to steric effects for reaction at phosphorus have been observed for bulky nucleophiles reacting with trimethyl phosphate; these nucleophiles react preferentially at carbon. In the gas phase, however, barriers due to steric effects for nucleophilic substitution are small;[63] thus, steric effects for reaction at phosphorus are probably not important for the gas-phase reactions of trimethyl phosphate.

One important reason that nucleophilic substitution at carbon is kinetically more favorable than nucleophilic substitution at phosphorus in the present study is that the substitution at carbon produces a much better leaving group than the substitution at phosphorus. If the nucleophile were to attack the phosphorus, it must extrude methoxide as the leaving group; on the other hand, if the nucleophile attacks the carbon, dimethyl phosphate anion is the leaving group. Methanol is much less acidic than dimethyl phosphate ($\Delta H°_{acid}$ = 381.7 kcal mol^{-1} and 332 kcal mol^{-1}, respectively), so in as much as weak bases indicate good leaving groups (both leaving groups are oxygen-centered anions), a direct displacement reaction at phosphorus may not compete with a direct displacement reaction at carbon simply because the dimethyl phosphate anion is a much better leaving group than methoxide. The reactions of anions with trimethyl phosphate in the gas phase are easily understood if we assume that there is a barrier to addition at phosphorus. The same leaving-group argument may be made in the liquid phase; however, phosphorus attack is observed in solution. In the condensed phase, therefore, solvation must be playing a specific role in making the phosphorus reaction pathway more facile than the carbon pathway.

For the reaction of amide with trimethyl phosphate, Hodges and co-workers[21] found three products, 5% CH_3O^-, 20% $(CH_3O)_2PO^-$, and 75% $(CH_3O)_2PO_2^-$, while, for the reaction of hydroxide with trimethyl phosphate, they found two products, 15% CH_3O^- and 85% $(CH_3O)_2PO_2^-$. In both reactions, the yield for methoxide represents a lower limit. They assigned the $(CH_3O)_2PO_2^-$ product anion to nucleophilic substitution at carbon, the $(CH_3O)_2PO^-$ product anion to elimination across C–O, and the CH_3O^- product anion to attack at phosphorus. It seems to us, however, that if attack by amide at phosphorus had occurred, then one should observe predominantly $(CH_3O)_2PONH^-$ rather than CH_3O^-, since CH_3O^- is expected to be a much stronger base than $(CH_3O)_2PONH^-$. From our data on the methoxide reaction, it is clear that if methoxide is produced, it reacts again before it leaves the complex, even if only a S_N2 pathway is open to it. Our data indicate that "free" methoxide is not produced from the thermally-equilibrated reaction of amide ion (or any ion for that matter) with trimethyl phosphate.

The gas-phase reactions of trimethyl phosphate that we have examined suggest that trimethyl phosphate is much more selective in its reaction with anions that other esters that we have studied. For example, for the reaction of CD_3O^- with trimethyl phosphate, the observed relative rate for nucleophilic substitution at carbon versus nucleophilic substitution at phosphorus is 43:1. In contrast, the data for the reaction of CD_3O^- with dimethyl sulfite[23] show that the relative rate for attack at carbon versus attack at sulfur is 1:1. For the reaction of methoxide-d_3 with trimethyl phosphite,[64] attack at carbon competes with attack at phosphorus. When methoxide-d_3 is allowed to react with methyl pyruvate,[25] methyl acetate,[24] or methyl thioacetate,[24] proton transfer predominates (>80%), while only a minor amount (<20%) of $B_{AC}2$ is observed. Therefore, for these methyl esters, even when a relatively facile proton transfer competes with an electrophilic substitution, the latter reaction channel is observed to some extent. In the examples discussed above, only trimethyl phosphate reacts with methoxide-d_3 to yield almost exclusively one product. The absence of significant products arising from phosphorus attack in trimethyl phosphate, as compared to these other cases, emphasizes the unusual stability of the phosphoryl group of trimethyl phosphate.

When we were examining the reactions of $(CH_3O)_2PO_2^-$ with Brönsted acids, we also looked for a methyl metaphosphate (CH_3OPO_2) transfer between the dimethyl phosphate anion and anions whose conjugate acids are slightly less acidic than dimethyl phosphate; one possible reaction is shown in eq 3 for HCl. We

$$(CH_3O)_2PO_2^- + HCl \nrightarrow (Cl)(CH_3O)PO_2^- + CH_3OH \qquad (3)$$

were unable, however, to find evidence for a methyl metaphosphate transfer between $(CH_3O)_2PO_2^-$ and any Brönsted acid we examined. An analogous tranfer of SO_2 was observed in the reactions of $CH_3OSO_2^-$ with several Brönsted acids.[23]

The reaction of hydroxide with trimethyl phosphate (EFF = 0.71) is less efficient than the reaction of hydroxide with trimethyl phosphite[64] (EFF = 0.93) in the gas phase. This same trend is also observed in solution, where trimethyl phosphite is hydrolyzed faster than trimethyl phosphate.[18] In solution, hydroxide reacts with both trimethyl phosphite and trimethyl phosphate at phosphorus, while, in the gas phase, hydroxide reacts with trimethyl phosphite exclusively at phosphorus and reacts with trimethyl phosphate almost exclusively at carbon.

Conclusions

Essentially two reaction pathways account for the reaction of a variety of anions possessing different structures and energetics with trimethyl phosphate: (i) nucleophilic substitution at carbon and (ii) reductive elimination across a carbon–oxygen bond. No significant products arising from a substitution process at phosphorus were found; however, when methoxide-d_3 and ethoxide were allowed to react with trimethyl phosphate, trace amounts of products resulting from substitution at phosphorus were observed. Only the strongest bases tried yielded elimination products, while every anion studied that displayed bimolecular reactivity yielded nucleophilic substitution products. The lack of a significant amount of labeled products from the reaction of methoxide-d_3 with trimethyl phosphate indicates that the formation of a pentacoordinate phosphorus intermediate is not on the reaction coor-

(62) Kirby, A. J.; Warren, S. G. In *The Organic Chemistry of Phosphorus*; Eaborn, C., Chapman, N. B., Eds.; Reaction Mechanisms in Organic Chemistry Monograph 5; Elsevier: New York, 1967.

(63) DePuy, C. H.; Gronert, S.; Mullin, A.; Bierbaum, V. M. *J. Am. Chem. Soc.* **1990**, *112*, 8650–8655. Gronert, S.; DePuy, C. H.; Bierbaum, V. M. *J. Am. Chem. Soc.* **1991**, *113*, 4009–4010. Olmstead, W. N.; Brauman, J. I. *J. Am. Chem. Soc.* **1977**, *99*, 4219–4228.

(64) Anderson, D. R.; DePuy, C. H.; Filley, J.; Bierbaum, V. M. *J. Am. Chem. Soc.* **1984**, *106*, 6513–6517.

dinate for substitution at phosphorus. The substitution reaction at carbon may dominate simply because it possesses a better leaving group than the substitution reaction at phosphorus. The acidity of dimethyl phosphate, whose conjugate base was the leaving group for the substitution reaction at carbon, was bracketed between those of hydrochloric acid and dichloroacetic acid, leading to $\Delta G°_{acid}[(CH_3O)_2PO_2H] = 325 \pm 4$ kcal mol^{-1} and $\Delta H°_{acid}[(CH_3O)_2PO_2H] = 332 \pm 4$ kcal mol^{-1}. The reactions of anions with trimethyl phosphate in the gas phase are unusual because they are very selective, yielding only products from reaction at carbon, which is in direct contrast to the reactions of phosphates in enzymes.

Acknowledgment. We gratefully acknowledge the support of this research by the National Science Foundation (Grant CHE-9196164). R.C.L. thanks Procter and Gamble for a fellowship administered by the Organic Division of the American Chemical Society.

Supplementary Material Available: Branching-ratio plots for the reactions of H_2N^-, $C_6H_5^-$, $PrNH^-$, and CD_3O^- with trimethyl phosphate, table of the results of acidity bracketing of $(CH_3O)_2PO_2^-$, and table of heats of formation used in this work (9 pages). Ordering information is given on any current masthead page.

Understanding Heterolytic Bond Cleavage

P. B. Armentrout*,† and Jack Simons*

Contribution from the Chemistry Department, University of Utah, Salt Lake City, Utah 84112.
Received July 19, 1991

Abstract: When considering the fragmentation of a single bond, the attractive singlet and repulsive triplet potential energy curves of the prototype $H_2 \rightarrow 2H$ dissociation often come to mind. For species in which homolytic bond cleavage is energetically favored, such comparisons are reasonable. For other species where heterolytic cleavage gives lower-energy products, the H_2 analogy is inappropriate. This paper offers a qualitative theoretical treatment of the singlet and triplet potential energy curves that arise when a single bond formed by an electron pair is cleaved either homolytically or heterolytically. This analysis is shown to provide insight into several problems involving transition metal systems: transition metal carbonyls, metal ion–ligand complexes, and transition metal dimers.

I. Introduction

As chemists, much of our intuition concerning chemical bonds is built on simple models introduced in undergraduate chemistry courses. The detailed examination of the H_2 molecule via the valence bond and molecular orbital approaches forms the basis of our thinking about bonding when confronted with new systems. Ordinarily, when we imagine bringing two radicals X$^\bullet$ and Y$^\bullet$ (each having a doublet spin state) together to form a single covalent bond, we anticipate that a bonding singlet state and a repulsive triplet state of the XY molecule are formed, much as they are for H_2. However, we have recently encountered several systems in which this picture of the bonding is incomplete and for which this simple intuition has led to flawed analyses involving qualitatively incorrect potential energy surfaces.

These cases involve species that dissociate heterolytically; i.e., during cleavage of a covalent bond one of the fragments retains both bonding electrons and these fragments have energies below those where each fragment retains a single electron. Far from being unusual, a preference for heterolytic bond cleavage arises quite naturally in systems involving transition metals, where interactions between empty metal orbitals and two-electron donor ligands are ubiquitous. This situation is qualitatively different from the case of H_2, where the $H^+ + H^-$ asymptote lies at much higher energies than H + H. The purpose of this paper is to outline how to correctly assess the qualitative characteristics of the potential energy surfaces involved in bonds that cleave heterolytically.

The theoretical methods and concepts included in this work are not new. Indeed, a series of articles by Pross and Shaik apply a valence-bond picture to explain the singlet-state potential energy surfaces that characterize a wide variety of prototypical organic reactions, including cation–anion recombination,[1] donor–acceptor interactions,[2,3] elmination reactions,[4] and solution-phase S_N2 reactions.[5] This previous work demonstrates that the ideas discussed here have a very broad applicability. In the present paper, the roles of spin and permutational symmetry in determining which asymptotic states connect to which states of the XY molecule are treated in more detail than in refs 1–5, and the results are directed at elucidating transition metal systems.

II. Summary of the State Correlations

To consider why the two-orbital, two-electron single bond formation case can be more complex than often thought, consider the H_2 system in detail. In the molecular orbital (MO) description of H_2, both bonding σ_g and antibonding σ_u MOs appear. There are two electrons that can both occupy the σ_g MO to yield the $^1\Sigma_g^+(\sigma_g^2)$ ground electronic state; however, they can also occupy both MOs to yield $^3\Sigma_u^+(\sigma_g^1\sigma_u^1)$ and $^1\Sigma_u^+(\sigma_g^1\sigma_u^1)$, or both can occupy the σ_u MO to give the $^1\Sigma_g^+(\sigma_u^2)$ state. As demonstrated explicitly in Appendix A, the former two states dissociate homolytically to X$^\bullet$ + X$^\bullet$ = H + H, and the latter two dissociate heterolytically to X + X:$^-$ = $H^+ + H^-$. (In all cases considered here, only two electrons play active roles in the bond formation. The symbols X, X$^\bullet$, and X:$^-$ are used to denote species in which neither, one, or both bonding electrons, respectively, are attached to the X fragment.) In the case of H_2 and for many other systems, the latter two states are sufficiently high in energy relative to the former two that they can be (and often are) ignored.

For several systems studied in our recent research, we have confronted situations where one of the heterolytic bond dissociation asymptotes (X + Y:$^-$ or X:$^-$ + Y) is *lower* in energy than the homolytic bond dissociation asymptote. In such cases, σ bonding and σ^* antibonding MOs are formed from the X and Y fragment

† Camille and Henry Dreyfus Teacher-Scholar, 1987–1992.

(1) Shaik, S. *J. Org. Chem.* **1987**, *52*, 1563.
(2) Shaik, S. *J. Am. Chem. Soc.* **1981**, *103*, 3692.
(3) Pross, A.; Shaik, S. *J. Am. Chem. Soc.* **1981**, *103*, 3702.
(4) Pross, A.; Shaik, S. *J. Am. Chem. Soc.* **1982**, *104*, 187.
(5) Pross, A.; Shaik, S. *Acc. Chem. Res.* **1983**, *16*, 363.

0002-7863/92/1514-8627$03.00/0